

## Dynamics of Ultrafast Phase Changes in Amorphous GeSb Films

K. Sokolowski-Tinten,<sup>1</sup> J. Solis,<sup>2</sup> J. Bialkowski,<sup>1</sup> J. Siegel,<sup>2</sup> C. N. Afonso,<sup>2</sup> and D. von der Linde<sup>1</sup>

<sup>1</sup>*Institut für Laser- und Plasmaphysik, Universität-GHS-Essen, D-45117 Essen, Germany*

<sup>2</sup>*Instituto de Optica, CSIC, C/Serrano 121, 28006 Madrid, Spain*

(Received 24 February 1998)

Time resolved imaging has been used to analyze structural transformations induced by intense 100 fs laser pulses in amorphous GeSb films. Above a threshold of 19 mJ/cm<sup>2</sup> the data show the formation of a transient nonequilibrium state of the excited material within 300 fs. The results are consistent with an electronically induced, amorphous-to-crystalline phase transition. [S0031-9007(98)07514-0]

PACS numbers: 61.80.Ba, 61.43.Dq, 68.35.Bs, 68.35.Rh

The existence of nonthermal, ultrafast phase transitions after strong femtosecond laser excitation has been demonstrated in several materials such as silicon [1–3], gallium arsenide [3–6], indium antimonide [7], and carbon [8]. It is accepted that such transitions are induced by a softening of the lattice structure due to the generation of a very high density electron-hole plasma, as first proposed by Van Vechten [9]. Most of the experimental and theoretical work [10–13] has concentrated on the solid-to-liquid phase transformation of the above mentioned materials. Some authors [2,11] have also claimed the existence of an ultrafast solid-to-solid phase transition preceding nonthermal melting, although there is experimental evidence [3,7] refusing this hypothesis.

In this Letter we present a time resolved study on the dynamics of femtosecond laser induced structural transformations in amorphous GeSb. We describe experimental evidence for the subpicosecond formation of a transient phase of the material and interpret our results as first indication for an ultrafast, nonthermal amorphous-to-crystalline phase transition. Sb-rich amorphous GeSb films can be crystallized upon irradiation with ultrashort laser pulses [14] and show a large optical contrast upon transformation [15]. This effect makes GeSb a promising material for the development of rewritable optical memories driven by ultrashort laser pulses [16]. Recently, it has been demonstrated [17] that the energy fluence necessary to induce crystallization in this material decreases significantly for pulses shorter than a picosecond, suggesting the relevance of electronic processes in the amorphous-to-crystalline transition.

Amorphous Ge<sub>0.06</sub>Sb<sub>0.94</sub>, 50-nm-thick films were grown on glass substrates at room temperature in a multitarget dc magnetron sputtering system from pure (99.999%) Ge and Sb targets. The films were irradiated with 100 fs laser pulses at 620 nm delivered by a 10-Hz amplified colliding-pulse mode-locked (rhodamine 6G/DODCI) dye laser. The evolution of the reflectivity of the irradiated surface was monitored with both femtosecond time and micrometer spatial resolution by means of ultrafast time-resolved microscopy [18]. A first laser pulse excites the sample. A second time-delayed probe pulse replaces the standard illumination of an

optical microscope and provides snapshot pictures of the excited surface with 100 fs time resolution. The optical micrographs are recorded with the help of a charged coupled device detector in conjunction with a computer controlled frame-grabber. Since a single laser pulse induces permanent structural changes of the irradiated area the sample is moved between two consecutive exposures.

A series of pictures, covering the entire period from the initial deposition of the laser energy (pump fluence 45 mJ/cm<sup>2</sup>) to the appearance of the final structural modifications, is shown in Fig. 1. The contrast of the images has been enhanced for reproduction purposes and thus Fig. 1 does not provide a quantitative measure of the evolution of the reflectivity. Because of the large angle between pump and probe (45°), the actual delay depends on the space coordinate along the horizontal axis of the images (100 fs/42 μm), but the delay is constant in the vertical direction (zero delay in Fig. 1 is referred to the center of the spot). Therefore, as the pump pulse sweeps across the surface from left to right, the fast subpicosecond increase in reflectivity ( $\Delta t = 250$  fs) is observed first on the left side of the irradiated spot, resulting in an asymmetric reflectivity pattern. This effect becomes negligible at longer delays. In the next frame ( $\Delta t = 1$  ps) the reflectivity of the whole irradiated region has increased giving rise to the appearance of an elliptical bright area without a sharply defined edge. On a tens-of-ps time scale ( $\Delta t = 20$  ps) a low reflectivity zone develops in the center of the spot. It subsequently disappears, leaving behind a bright ellipse with a sharply defined boundary ( $\Delta t = 200$  ps). The appearance of the irradiated surface area remains nearly unchanged up to approximately 1 ns ( $\Delta t = 900$  ps), when the reflectivity of the outermost region starts to decrease ( $\Delta t = 10$  ns). At even later times a different high reflectivity region begins to form ( $\Delta t = 29$  ns). High reflectivity in this region becomes permanent as can be seen in the last frame ( $\Delta t = \infty$ ), corresponding to a delay of several seconds.

Because of the Gaussian intensity distribution of the focused pump beam, different spatial locations represent the behavior of the reflectivity for different pump fluences. Any sharp boundary in the images shown in Fig. 1 therefore indicates the existence of a well-defined threshold.

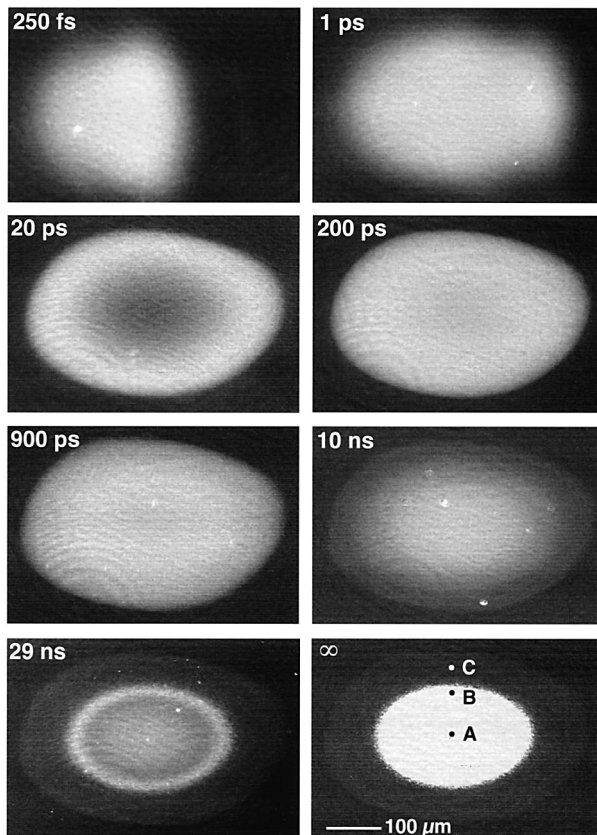


FIG. 1. Pictures of an amorphous GeSb surface at different times after exposure to the pump pulse (pump fluence  $45 \text{ mJ/cm}^2$ ).

The edge of the large ellipse with increased reflectivity observed at  $\Delta t = 200 \text{ ps}$  corresponds to a threshold fluence of  $5 \text{ mJ/cm}^2$ . The position of this edge coincides with the outer boundary of the final transformed region ( $\Delta t = \infty$ ), which can be recognized by a slight reflectivity increase compared to the initial reflectivity. The permanent high reflectivity phase seen in the same frame (bright ellipse) is observed only above  $19 \text{ mJ/cm}^2$ .

To quantitatively follow the time evolution, we have plotted in Fig. 2 the absolute reflectivity (absolute error  $\approx 0.005$ ) as a function of delay time, as measured in three different locations (marked as A, B, and C in the frame  $\Delta t = \infty$  in Fig. 1). Trace A represents the time dependence at maximum fluence ( $45 \text{ mJ/cm}^2$ ). Traces B and C correspond to fluences of 20 and  $12 \text{ mJ/cm}^2$ , respectively, slightly above and well below the threshold for the appearance of the final high reflectivity phase. At the highest fluence (curve A) the reflectivity increases to a maximum value of 0.71 in less than a picosecond. Then it decreases slowly towards a minimum at  $\Delta t \approx 20 \text{ ps}$  and rises again reaching values of 0.68 and 0.69 in about 200 ps and 2 ns, respectively. The reflectivity remains then nearly constant up to about 10 ns. A second reflectivity minimum is observed at  $\Delta t \approx 30 \text{ ns}$ , followed by a final increase to a stationary value of 0.71. Trace B shows a similar

behavior, although the first minimum is less pronounced and the period of nearly constant reflectivity ( $R \approx 0.69$ ) lasts for a shorter time. Trace C, measured outside the region of permanent high reflectivity, is characterized by an initial subpicosecond increase, which *does not* reach  $R = 0.71$ . Instead, the reflectivity slowly rises up to 0.69 in 30 ps and stays then constant up to about 100–150 ps. Subsequently, it starts to decrease reaching a stationary level of  $R = 0.59$  after 30 ns.

The reflectivity of the liquid and crystalline phase of Sb-rich GeSb is known at  $633 \text{ nm}$  [15,19] and nearly identical to that of pure Sb (*l*-Sb:  $R = 0.67$ , *c*-Sb:  $R = 0.71$ , [20]). The reflectivity of the amorphous phase is significantly lower,  $R = 0.57\text{--}0.58$ , slightly dependent on composition and state of structural relaxation [21]. Thus the observation of a nearly constant reflectivity level with  $R \approx 0.69$  in the ps to ns time domain for fluences above  $5 \text{ mJ/cm}^2$  can be attributed to melting of the material over a thickness larger than the penetration depth of the probe pulse radiation. The final reflectivity of 0.71 observed above  $19 \text{ mJ/cm}^2$  (traces A and B) indicates the formation of crystalline material upon solidification, while between 5 and  $19 \text{ mJ/cm}^2$  the resolidified material is amorphous (trace C). The slight difference between initial and final reflectivity of the amorphous is related to differences in its state of structural relaxation [21]. The nanosecond behavior of the reflectivity above the crystallization threshold  $F_{\text{cr}} = 19 \text{ mJ/cm}^2$  is quite similar to what has been measured on GeSb films irradiated with ns and ps pulses [15,19]. In particular the reflectivity minimum observed in the tens of ns time scale in traces A and B is related to bulk nucleation of amorphous material within the molten

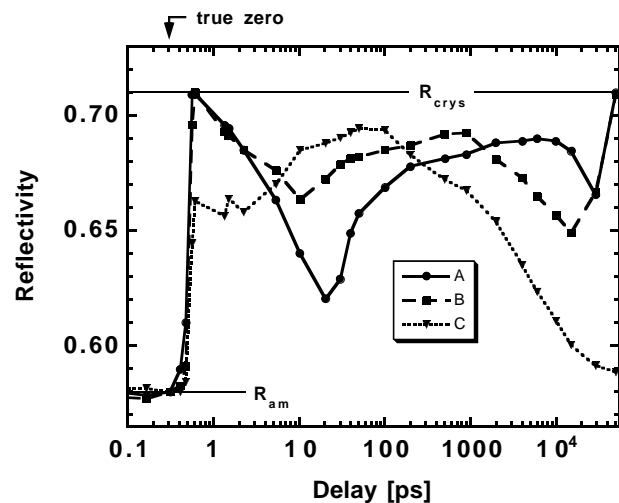


FIG. 2. Reflectivity as a function of delay time measured at three different locations (marked as A, B, and C in the last frame of Fig. 1), corresponding to excitation fluences of 45, 20, and  $12 \text{ mJ/cm}^2$ , respectively. The rightmost data point of each curve represents the final reflectivity ( $\Delta t = \infty$ ). Note the logarithmic time axis; the true zero delay (see text) is marked by an arrow.

volume during the initial stage of solidification. The release of the solidification enthalpy reduces then the undercooling of the melt promoting further solidification in the crystalline phase, accompanied by an increase of the reflectivity. This *frustrated amorphization* process has been described in detail in Ref. [15]. At lower fluences (trace C) the undercooling prior to solidification is higher. This favors solidification in the amorphous phase, similar to what has been observed in elementary semiconductors [22].

At low fluences (trace C) the fast rise of reflectivity can be ascribed to the primary excitation process, i.e., creation of a dense electron-hole plasma. After the thermalization of the carrier energy the reflectivity increases to a value of 0.69 within 30 ps, indicating thermal melting of the material [6]. Above  $F_{cr}$  (traces A and B) the reflectivity shows an initial increase to a maximum value of 0.71 on a subpicosecond time scale, passes through a minimum ( $\approx 20$  ps) and reaches later the value of the normal molten phase. Similar to what is known from laser molten silicon [23], the apparently fluence dependent reduction of reflectivity might be related to temperature dependent changes of the optical constants of the liquid material.

The subpicosecond behavior of the reflectivity in traces A and B is remarkable for two reasons. The attained maximum reflectivity is (1) identical to the reflectivity of crystalline GeSb, and (2) independent on pump fluence whenever  $F_{cr}$  is exceeded. Vertical cross sections of the time resolved snapshots from Fig. 1 confirm these conclusions. In Fig. 3 reflectivity is plotted for three representative delays (250 fs, 200 ps, and  $\infty$ ) as a function of the distance to the center of the spot, and thus as a function of the local pump fluence. The trace for  $\Delta t = \infty$  shows a plateau with a value of 0.71, corresponding to the region finally crystallized. The trace for  $\Delta t = 200$  ps with top reflectivity values around 0.68–0.69 (lower in the center of the spot) shows the formation of an optically thick layer of hot, liquid material, as discussed above. The flattop behavior at  $\Delta t = 250$  fs, clearly demonstrating the fluence independence of the reflectivity, excludes that the excited electron-hole plasma is responsible for the observed change in reflectivity, but is a clear indication of a transient *phase* of the material. A comparison of the reflectivity profiles for  $\Delta t = 250$  fs and  $\Delta t = \infty$  shows that the reflectivity of the transient phase is exactly equal to that of the crystalline state. Moreover, the transient phase is observed only in the very region in the center of the excited area where (final) crystallization takes place.

Our data show that the dynamics of phase transformations in *a*-GeSb under fs excitation is significantly different from that observed in group IV and III-V semiconductors. For the latter a subpicosecond solid-to-liquid transition occurs and the liquid resulting from nonthermal melting exhibits the same optical properties as the equilib-

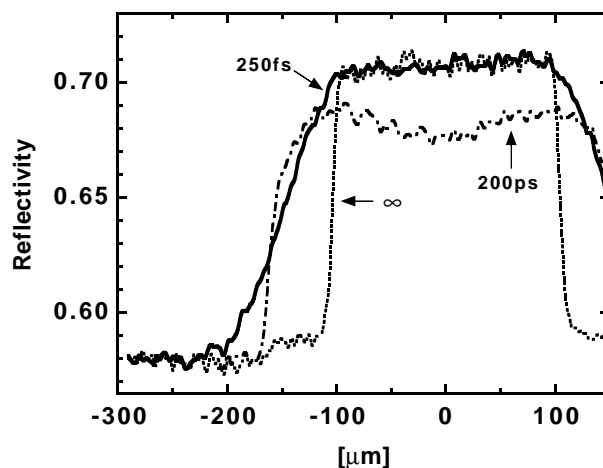


FIG. 3. Vertical cross sections of the time resolved snapshot pictures in Fig. 1 for delay times of  $\Delta t = 250$  fs, 200 ps, and  $\infty$ : Reflectivity as function of the distance to the center of the excited spot (fluence dependence).

rium molten phase [3,12]. In *a*-GeSb the observed time scale ( $\approx 300$  fs) also evidences a nonthermal process, but the transient phase is *not* the normal molten phase. Although we cannot completely rule out the existence of an intermediate, *different*, nonequilibrium liquid state, Fig. 3 gives strong experimental evidence for a connection between the transient phase and the crystalline state of the material.

To explain these observations we propose a scenario in which for fluences above  $19 \text{ mJ/cm}^2$  an electronically induced, nonthermal *amorphous-to-crystalline* phase transformation occurs before the material melts. Several arguments suggest that Sb-rich GeSb is a candidate for such an ultrafast solid-to-solid phase transition. (1) The structure of the crystalline phase obtained upon rapid solidification is that of pure Sb [15]. The amorphous phase originates from small distortions of the crystal, which destroy long range order, but leave the microstructure essentially unchanged. (2) In pure Sb coherent phonons can be easily generated by fs-laser excitation via the so-called *displacive excitation* mechanism [24]. The potential minima, which define the equilibrium structure of the lattice, are *displaced* in the presence of a dense electron-hole plasma. This initiates atomic relaxation towards the new quasiequilibrium configuration of the material. It is therefore possible that in the amorphous phase electronic excitation also leads to *displaced* potentials and thus to vibrational motion. Provided that in the amorphous phase the atoms are close to the crystalline ordered configuration, the electronically induced atomic motion might be sufficient to enable a transformation to a crystalline or, more likely, to a *nanocrystalline* or *microquasicrystalline* state [25] within a few hundred femtoseconds. Notice that in metals and semimetals a grain size in the nm range [26] is sufficient to observe the optical properties of the crystalline phase.

Some further conclusions can be drawn from Fig. 3. Obviously the solidification behavior in the area undergoing the nonthermal phase change and in the regions irradiated at lower fluences are significantly different. In both cases an optically thick layer of liquid material is formed within 10–20 ps. Subsequently this layer becomes undercooled and solidifies. The degree of undercooling determines the structure of the solidified material (amorphous or crystalline) and depends not only on the local pump fluence but also on the initial nucleation behavior [27,28]. The density of initial nuclei is strongly influenced by the thermal and structural history of the system [29] which therefore determines the subsequent early nucleation stage, the attainable undercooling, and the final result of the solidification process. This might explain how the material *remembers* the spatial region in which the subpicosecond phase transition was induced.

In conclusion, we have investigated the dynamics of femtosecond laser induced phase transformations in amorphous GeSb. We found compelling evidence for a transient phase of the excited material, which is observed for only a few hundred femtoseconds and shows a striking similarity to crystalline GeSb. Our data can be interpreted as an indication for an electronically induced amorphous-to-crystalline phase transformation.

K. S. T. acknowledges support by the *Flughafen Frankfurt Main* foundation and by the University of Essen (*Forschungspool*). J.S. acknowledges funding by the European Community (*Training and Mobility of Researchers*, ERB 40001GT954352). This work has been partially supported by CICYT (Spain, TIC93-0125).

- 
- [1] C. V. Shank, R. Yen, and C. Hirlimann, *Phys. Rev. Lett.* **50**, 454 (1983); **51**, 900 (1983).
- [2] H. W. K. Tom, G. D. Aumiller, and C. H. Brito-Cruz, *Phys. Rev. Lett.* **60**, 1438 (1988).
- [3] K. Sokolowski-Tinten, J. Bialkowski, and D. von der Linde, *Phys. Rev. B* **51**, 14 186 (1995).
- [4] S. V. Govorkov, T. Schröder, I. L. Shumay, and P. Heist, *Phys. Rev. B* **46**, 6864 (1992).
- [5] P. Saeta, J.-K. Wang, Y. Siegal, N. Bloembergen, and E. Mazur, *Phys. Rev. Lett.* **67**, 1023 (1991); E. N. Glezer, Y. Siegal, L. Huang, and E. Mazur, *Phys. Rev. B* **51**, 9589 (1995); L. Huang, J. P. Callan, E. N. Glezer, and E. Mazur, *Phys. Rev. Lett.* **80**, 185 (1998).
- [6] K. Sokolowski-Tinten, H. Schulz, J. Bialkowski, and D. von der Linde, *Appl. Phys. A* **53**, 227 (1991).
- [7] I. L. Shumay and U. Höfer, *Phys. Rev. B* **53**, 15 878 (1996).
- [8] D. H. Reitze, H. Ahn, and M. C. Downer, *Phys. Rev. B* **45**, 2677 (1992).
- [9] J. A. Van Vechten, R. Tsu, and F. W. Saris, *Phys. Lett.* **74A**, 422 (1979).
- [10] S. Das Sarma and J. R. Senna, *Phys. Rev. B* **49**, 2443 (1994).
- [11] P. Stampfli and K. H. Bennemann, *Phys. Rev. B* **42**, 7163 (1990); **46**, 10 686 (1992); **49**, 7299 (1994).
- [12] P. L. Silvestrelli, A. Alavi, M. Parrinello, and D. Frenkel, *Phys. Rev. Lett.* **77**, 3149 (1996).
- [13] J. S. Graves and R. E. Allen (to be published).
- [14] C. N. Afonso, J. Solis, F. Catalina, and C. Kalpouzou, *Appl. Phys. Lett.* **60**, 3123 (1992).
- [15] J. Solis, C. N. Afonso, J. F. Trull, and M. C. Morilla, *J. Appl. Phys.* **75**, 7788 (1994).
- [16] M. C. Morilla, J. Solis, and C. N. Afonso, *Jpn. J. Appl. Phys. Pt. 2*, **36**, L1015 (1997).
- [17] J. Solis, C. N. Afonso, S. C. W. Hyde, N. P. Barry, and P. M. W. French, *Phys. Rev. Lett.* **76**, 2519 (1996).
- [18] M. C. Downer, R. L. Fork, and C. V. Shank, *J. Opt. Soc. Am. B* **4**, 595 (1985).
- [19] C. N. Afonso, M. C. Morilla, J. Solis, N. H. Rizvi, M. A. Ollacarizqueta, and F. Catalina, *Mater. Sci. Eng. A* **173**, 343 (1996).
- [20] R. Serna, J. Solis, and C. N. Afonso, *J. Appl. Phys.* **73**, 3099 (1993).
- [21] M. C. Morilla, C. N. Afonso, and J. Solis, *Appl. Phys. A* **62**, 559 (1996).
- [22] M. O. Thompson, J. W. Mayer, A. G. Cullis, H. C. Webber, N. G. Chew, J. M. Poate, and D. C. Jacobson, *Phys. Rev. Lett.* **50**, 896 (1983).
- [23] J. Boneberg, O. Yavas, B. Mierswa, and P. Leiderer, *Phys. Status Solidi (b)* **174**, 295 (1992).
- [24] H. J. Zeiger, J. Vidal, T. K. Cheng, E. P. Ippen, G. Dresselhaus, and M. S. Dresselhaus, *Phys. Rev. B* **45**, 768 (1992).
- [25] L. C. Chen and F. Spaepen, *Nature (London)* **336**, 366 (1988).
- [26] Z. Pan, S. H. Morgan, D. O. Henderson, S. Y. Park, R. A. Weeks, R. H. Magruder III, and R. A. Zuhr, *Opt. Mater.* **4**, 675 (1995).
- [27] W. J. Boettinger and J. H. Perepezco, *Fundamentals of Rapid Solidification in Rapidly Solidified Crystalline Alloys*, edited by S. K. Das, B. H. Kear, and C. M. Adam (The Metallurgical Society, Warrendale, PA, 1985).
- [28] L. A. Jacobson and J. McKittrick, *Mater. Sci. Eng.* **R11**, 355 (1994).
- [29] K. F. Kelton, A. L. Greer, and C. V. Thompson, *J. Chem. Phys.* **79**, 6262 (1983).